New renormalization equations for the Kosterlitz-Thouless transition

Petter Minnhagen
Department of Theoretical Physics, University of Umeå, S-90187 Umeå, Sweden
(Received 5 April 1985)

A new set of renormalization equations for the two-dimensional Coulomb gas is derived and solved numerically. These equations give a new picture of the Kosterlitz-Thouless transition. A new temperature T^* is found. Above T^* the value of the dielectric constant at the transition is $\epsilon_c = 1/(4T_c)$ as before whereas below T^* the new result $\epsilon_c < 1/(4T_c)$ is obtained. The singular behavior at T^* is explored. The results are translated into a renormalization-group flow diagram. An interesting consequence is that the universal jump prediction for the Kosterlitz-Thouless transition turns into a nonuniversal jump prediction for critical temperatures below T^*.

I. INTRODUCTION

A new set of renormalization equations for the Kosterlitz-Thouless[1,2] transition of a two-dimensional Coulomb gas is presented. A short description of the work has been given earlier.[3] In the present paper we give a more complete account with detailed derivations.

The Kosterlitz-Thouless transition is of interest in a variety of contexts.[4] The present work has implications for two-dimensional (2D) XY models and to superfluid and superconducting films. An interesting consequence of the Kosterlitz-Thouless transition for these cases is that the helicity modulus[5] or equivalently, the superfluid density[6,7] jumps discontinuously from a finite value to zero at the transition. The size of the jump was deduced by Nelson and Kosterlitz[6] from the lowest-order renormalization-group (RG) equations[8] together with an assumption for the structure of the RG flow diagram. This prediction for the size of the jump will be referred to as the universal jump prediction. The new equations give a different RG flow diagram than that assumed in the universal jump prediction. As a consequence the universal jump turns into a nonuniversal jump below a certain temperature. Possible candidates for systems undergoing Kosterlitz-Thouless transitions with nonuniversal jumps are the half-frustrated 2D XY models on a square and honeycomb lattice. Some empirical evidence supporting the nonuniversal jump alternative for these models has been presented separately.[9]

The organization of the paper is as follows. In Sec. II we define the Coulomb-gas (CG) model and discuss the lowest-order RG equations from the point of view of a length-dependent dielectric constant. The purpose of this section, apart from introducing notations, is to provide a perspective, in which the new equations will be discussed later in the paper. In Sec. III we describe the connection to a sine-Gordon field-theory formulation and give the field-theory analog of the charge-density correlations and the linearly screened potential. With these prerequisites the derivation of the new equations is described in Sec. IV. A physical interpretation of the equations in terms of polarization due to dipole pairs is discussed in Sec. V. A numerical solution of the equations is presented in Sec. VI, while Sec. VII contains a discussion of the results. In addition some parts of the more detailed derivations are relegated to Appendixes A—C.

II. THE 2D COULOMB GAS AND LOWEST-ORDER RENORMALIZATION

A Coulomb gas (CG) consists of positive and negative charges of equal magnitude.[10] The charges interact through the Coulomb interaction which is defined by Poisson's equation

$$\nabla^2 V(r) = -2\pi f_\xi(\mathbf{r}) \tag{2.1}$$

(the unit of charge is taken to be 1). The length ξ is the linear dimension of a charge and will serve as an ultraviolet cutoff; more precisely the charge distribution of a single charge is given by some function $f_\xi(\mathbf{r})$, where

$$\lim_{\xi\to 0} f_\xi(\mathbf{r}) = \delta(\mathbf{r}) \; .$$

In two dimensions the Coulomb interaction depends logarithmically on distance, i.e.,

$$V(\mathbf{r}) \sim \ln(r) \; . \tag{2.2}$$

For the point-charge model, for which $f_\xi(\mathbf{r}) = \delta(\mathbf{r})$, the charges of opposite sign collapse into each other for small enough temperatures in two dimensions;[11] the point-charge model does not undergo a Kosterlitz-Thouless transition. However, the precise form of $f_\xi(\mathbf{r})$ will be of little importance in the following, apart from introducing an ultraviolet cutoff.

The 2D-CG is defined through the particle interaction and the grand-partition function Z,[10]

$$Z = \mathrm{Tr}(e^{-H/T}) = \sum_{N=0}^{\infty} \prod_i \int \frac{d\mathbf{r}_i}{\xi^2} e^{-H_N/T} \left[\left[\frac{N}{2} \right] ! \right]^{-2} . \tag{2.3}$$

Here N is the number of particles in a neutral configuration (a configuration with as many positive as negative charges), the index i numbers the particles in a configuration, $\mathbf{r}_i$ is a two-dimensional vector giving the particle position, ξ^2 is a phase-space division, T is the temperature (Boltzmann's constant is set to 1), and H_N is the configuration energy:

$$H_N=\frac{1}{2}\sum_{\substack{i,j\\(i\neq j)}} s_i s_j[U(r_{ij})-U(0)]-NT\ln z\ , \tag{2.4}$$

where r_{ij} is the distance between particles i and j, $U(r_{ij})$ is the interaction energy

$$U(r_{ij})=\int d^2r\, f_\xi(\mathbf{r}_i-\mathbf{r})V(|\mathbf{r}-\mathbf{r}_j|)\ ,$$

$U(0)/2$ is the electrostatic self-energy of a particle, $s_i=\pm1$ is the charge of a particle, and z is the particle fugacity. The fugacity is related to the chemical potential μ by $z=\exp(\mu/T)$. The interaction term $U(r)-U(0)$ is to leading order equal to $\ln(\xi/r)$ for $r/\xi\gg1$. Only neutral configurations contribute to the grand-partition function because the particle self-energy $U(0)/2$ is infinite.[10]

Our object is to find a description of the Kosterlitz-Thouless transition for this model with temperature T and fugacity z as variables. A key quantity in our reasoning will be the linearly screened potential (per unit charge), $V_L(r)$. It may be defined in the following way: Introduce into the CG two test particles with opposite infinitesimal charges, δs, separated by a distance r; $V_L(0)-V_L(r)$ is the interaction energy between the test particles divided by $(\delta s)^2$. In the absence of the CG, $V_L(r)$ is just the "bare" Coulomb interaction $V_L^{(0)}(r)$ which in Fourier space is given by

$$V_L^{(0)}(k)=\frac{2\pi}{k^2}\ . \tag{2.5}$$

In the presence of the CG, V_L is polarized and screened by the Coulomb-gas charges. This effect may be described by a dielectric function ϵ,

$$V_L(k)=V_L^{(0)}(k)/\epsilon(k)=2\pi/[k^2\epsilon(k)]\ . \tag{2.6}$$

The dielectric function ϵ is related to the charge-density correlations of the CG,

$$1/\epsilon(k)=1-\frac{2\pi}{Tk^2}\langle n(\mathbf{k})n(-\mathbf{k})\rangle\ , \tag{2.7}$$

where $n(\mathbf{k})$ is the Fourier transform of the CG charge density. The charge density for a configuration of N particles is given by

$$n(\mathbf{r})=\frac{1}{\Omega}\sum_{i=1}^{N}s_i f_\xi(\mathbf{r}-\mathbf{r}_i)\ , \tag{2.8}$$

where Ω is the volume. The angular brackets in Eq. 2.7, $\langle\ \rangle$, stand for a thermal average in the grand canonical ensemble defined by the grand-partition function Z [given by Eq. (2.3)].

The Kosterlitz-Thouless transition is reflected in V_L in the following way:[10] On the low-temperature side of the transition V_L is polarized but not screened (the screening length λ is infinite). The leading behavior of V_L for small k is given by

$$V_L(k)=\frac{2\pi}{\epsilon_0 k^2}\ , \tag{2.9a}$$

where

$$\epsilon_0\equiv\lim_{k\to0}\epsilon(k)\ . \tag{2.9b}$$

On the high-temperature side of the transition V_L is screened (i.e., λ is finite) and the leading behavior for small k is

$$V_L(k)=\frac{1}{\epsilon_a}\frac{1}{k^2+\lambda^{-2}}\ , \tag{2.10}$$

where ϵ_a is a constant describing the polarization. Note that $\epsilon_0=\infty$ on the high-temperature side [compare Eqs. (2.6), (2.9b), and (2.10)]. It follows that, precisely at the transition, the quantity $1/\epsilon_0$ jumps from a finite value, denoted by $1/\epsilon_c$, to zero. This jump and the quantity ϵ_c will play an important role in the following.

Now, since

$$\lim_{k\to0}\frac{1}{\epsilon(k)}=\frac{1}{\epsilon_0}$$

exists and is finite, it follows that

$$\lim_{k\to0}\frac{2\pi}{k^2}\langle n(k)n(-k)\rangle$$

also exists and is finite [compare Eq. (2.7)]. Consequently one has the following identity:

$$\lim_{k\to0}\frac{1}{k^2}\langle n(k)n(-k)\rangle=\frac{1}{2}\frac{\partial^2}{\partial k^2}\langle n(k)n(-k)\rangle\Big|_{k=0} \tag{2.11}$$

and thus

$$\begin{aligned}\frac{1}{\epsilon_0}&=1-\frac{2\pi}{2Tk^2}\frac{\partial^2}{\partial k^2}\int dr\,d\phi\, re^{ikr\cos\phi}\langle n(r)n(0)\rangle\Big|_{k=0}\\&=1+\frac{\pi}{T}\int dr\,d\phi\, r^3\cos^2\phi\langle n(r)n(0)\rangle\\&=1+\frac{\pi^2}{T}\int_0^\infty dr\, r^3\langle n(r)n(0)\rangle\ .\end{aligned} \tag{2.12}$$

In the intuitive picture of the Kosterlitz-Thouless transition, the low-temperature phase consists of dipole pairs.[1] One may interpret Eq. (2.12) within this picture in the following way: The density of dipole pairs with separation r, $\mathscr{D}_{\rm dip}(r)$, is given by

$$\mathscr{D}_{\rm dip}(r)=-\frac{\langle n(r)n(0)\rangle}{2}\Omega\ . \tag{2.13}$$

[The minus sign arises because the charges in a dipole have opposite sign and $\langle n(r)n(0)\rangle$ is the charge-density correlation. The factor $\frac{1}{2}$ arises because

$$\int d^2r d^2r'\langle n(r)n(r')\rangle$$

counts every pair twice.] The polarizability of a single dipole pair with separation r, $\alpha(r)$, is $\alpha(r)=r^2/2T$. One may then define an electric susceptibility, χ_0, corresponding to an "independent dipole-pair approximation"

$$\begin{aligned}\chi_0&=\frac{1}{\Omega}\int d^2r\,\alpha(r)\mathscr{D}_{\rm dip}(r)\\&=-\frac{\pi}{2T}\int_0^r dr\, r^3\langle n(r)n(0)\rangle\ .\end{aligned} \tag{2.14}$$

In terms of this quantity we may express the dielectric constant ϵ_0 as

$$\frac{1}{\epsilon_0}=1-2\pi X_0 . \tag{2.15}$$

In usual electrostatics one would have

$$\epsilon_0=1+2\pi X \tag{2.16}$$

in terms of the actual electric susceptibility and hence

$$X=\frac{X_0}{1-2\pi X_0} . \tag{2.17}$$

One notes that $X_0<\frac{1}{2}\pi$ in the low-temperature phase and $X_0=\frac{1}{2}\pi$ in the high-temperature phase.

The point of the above reasoning is that one may understand ϵ_0 in the low-temperature phase as being caused by polarization due to dipoles of all length scales. To get a feeling for how dipoles of different length scales contribute to ϵ_0 one may introduce a length-dependent dielectric function $\tilde{\epsilon}$ by

$$\frac{1}{\tilde{\epsilon}(r)}=1+\frac{\pi^2}{T}\int_0^r dr'\,r'^3\langle n(r')n(0)\rangle . \tag{2.18}$$

One notes that $\tilde{\epsilon}(r)$ involves all dipole pairs up to the separation r and that $\tilde{\epsilon}(\infty)=\epsilon_0$. One ingredient in the present paper will be to express $V_L(r)$ in terms of $\tilde{\epsilon}(r)$. The result may be expressed in terms of the mutual force F acting between the test particles

$$F(r)=-\frac{\partial}{\partial r}V_L(r) . \tag{2.19a}$$

In the absence of the CG this force is given by $F_0=1/r$. In Sec. IV we will make use of the following expression for the force F which follows directly from Eqs. (2.6), (2.7), and (2.18) (see Appendix B)

$$F(r)=F_1(r)+F_2(r)+F_3(r) , \tag{2.19b}$$

$$F_1(r)=1/r\tilde{\epsilon}(r) \tag{2.19c}$$

$$F_2(r)=\frac{r\pi^2}{T}\int_r^\infty dr'\,r'\langle n(r')n(0)\rangle , \tag{2.19d}$$

$$F_3(r)=\frac{2\pi^2 r}{T}\int_r^\infty dr'\,r'\ln(r'/r)\langle n(r')n(0)\rangle . \tag{2.19e}$$

A physical interpretation will be given in Sec. V. The point to note is that F involves contributions both from dipole pairs with separations smaller than the test-pair separation (F_1) and from dipole pairs with separations larger than the test-pair separation (F_2 and F_3).

In the original argument by Kosterlitz and Thouless[1] and the later improvements by Young[12] only dipole pairs smaller than the test pair were included. The point of Young's improvements[12] was to demonstrate that this "smaller dipole approximation" leads directly to Kosterlitz RG equations.[8] We will reproduce the argument below in order to get the connection to the present work precise.

The point of the present paper is to show that the inclusion of dipole pairs with separations larger than the test pair will, in fact, add qualitative new features to the Kosterlitz-Thouless transition.

The argument within the "smaller dipole approximation" goes as follows:[10,12] The force acting between a dipole pair of CG particles separated by a large distance r is, within this approximation, given by $F_1(r)=1/r\tilde{\epsilon}(r)$, i.e., the force is polarized by the smaller dipole pairs and this effect is taken into account by a length-dependent dielectric constant.[1,12] The interaction energy relative to the situation when the particles are separated by a distance ξ is then approximately

$$U_{\rm dip}(r)=\int_\xi^r dr'\frac{1}{r'\tilde{\epsilon}(r')} . \tag{2.20}$$

The effective Boltzmann factor for finding a dipole pair separated by a distance r is approximately $z^2\exp[-U_{\rm dip}(r)/T]$. The phase space available for a pair with the separation in the interval $[r,r+dr]$ is $\Omega 2\pi dr/\xi^4$ and the density of dipole pairs with separation r is thus (per orientational angle)

$$\mathscr{D}_{\rm dip}(r)\approx\frac{\Omega}{\xi^4}z^2\exp[-U_{\rm dip}(r)/T] , \tag{2.21}$$

which using Eq. (2.13) gives

$$\langle n(r)n(0)\rangle\approx-\frac{2}{\xi^4}z^2\exp[-U_{\rm dip}(r)/T] . \tag{2.22}$$

The key feature is now that Eqs. (2.18), (2.20), and (2.22) constitute a self-consistent set. By introducing a logarithmic length scale $l=\ln(r/\xi)$ and a length-dependent fugacity

$$z(l)=z\exp[2l-U_{\rm dip}(r)/2T] ,$$

this set of equations may be expressed in differential form as[10,12]

$$\frac{d}{dl}\frac{1}{T\tilde{\epsilon}(l)}=-\frac{2\pi^2 z^2(l)}{T^2} , \tag{2.23a}$$

$$\frac{d}{dl}z(l)=\frac{z(l)}{2}\left[4-\frac{1}{T\tilde{\epsilon}(l)}\right] . \tag{2.23b}$$

These equations will be referred to as the lowest-order RG equations. The quantity $\epsilon_0=\tilde{\epsilon}(\infty)$ may now be obtained by integrating Eqs. (2.23) from some known initial condition. For $l=0$ one has $z(l=0)=z$ and $\epsilon(l=0)\approx1$, where the last approximate equality rests on the assumption that there are few pairs with separation of the order of ξ. This approximation is, of course, both dependent on the single-particle charge distribution, $f_\xi(r)$, and on T. We will in the following assume that $f_\xi(r)$ is such that $\tilde{\epsilon}(l=0)\approx1$ always holds and will supplement our renormalization equations in the present paper with the initial conditions $z(0)=z$ and $\tilde{\epsilon}(0)=1$.

Some further perspective on this condition is given by the following example. Suppose that the charges are unimpenetrable disks with diameter ξ. As the temperature is lowered for constant z the separation of pairs decreases. The smallest separation distance is ξ which corresponds to the polarizability $\alpha(\xi)=\xi^2/2T$. Thus, for small T, χ_0 may be estimated by $\chi_0 \approx z^2/2T$ for small z. This means that for a fixed small z there will always be a phase transition at a temperature defined by the condition $\chi_0 = \frac{1}{2}\pi$. Consequently, the Kosterlitz-Thouless phase line will start at (0,0) in the (T,z) plane. It follows that the Kosterlitz-Thouless transition for the hard-disk model will always have a reentrant behavior.

However, for the soft cutoff models for which $\tilde{\epsilon}(l=0) \approx 1$, considered in the present paper, no such reentrant behavior is found. We believe that the soft cutoff implied by $\tilde{\epsilon}(l=0) \approx 1$ is the relevant one in connection with XY models and superfluid and superconducting films. An explicit calculation of $f_\xi(r)$ in connection with superconducting films is given in Ref. 13.

The object of the present paper is to find approximate renormalization equations which are valid outside the range $T \approx \frac{1}{4}$ and $z \approx 0$. To leading order in $T - \frac{1}{4}$ and z the lowest-order RG equations quoted in the literature are, of course, all equivalent. However, the nonleading terms are different. The equations by José *et al.*[14] and by Young[12] correspond to the approximation

$$\chi = \frac{\chi_0}{1 - 2\pi \chi_0} \approx \chi_0$$

This approximation changes Eq. (2.13a) to

$$\frac{d}{dl}[T\tilde{\epsilon}(l)] = 2\pi^2 z^2(l) \; .$$

On the other hand, the Kosterlitz renormalization procedure[8] leads precisely to Eq. (2.13). The RG equations may also be obtained through a sine-Gordon field-theory formulation.[15,16]

The lowest-order RG equations obtained by this approach also correspond to Eqs. (2.23). In Sec. IV we will rederive Eqs. (2.23) as the lowest-order equations by yet another approach. This leads us to believe that, from the point of view of obtaining an approximation outside the range $T \approx \frac{1}{4}$, Eqs. (2.23) constitute the best set to leading order in z.

Equations (2.23) are easily integrated into[8]

$$\left[\frac{1}{T} - 4\right]^2 - \frac{4z^2\pi^2}{T^2} = \left[\frac{1}{T\epsilon_0} - 4\right]^2 \tag{2.24}$$

valid for $\epsilon_0 T < \frac{1}{4}$. The phase transition is given by $\epsilon_0 T = \frac{1}{4}$ (Refs. 8 and 10) or

$$z = \frac{2}{\pi}\left(\tfrac{1}{4} - T\right) \; . \tag{2.25}$$

In Ref. 16 the next-order RG equations are obtained to leading orders in $\frac{1}{4} - T$ and z for an explicit soft cutoff procedure. Transcribed to the present notation these equations are

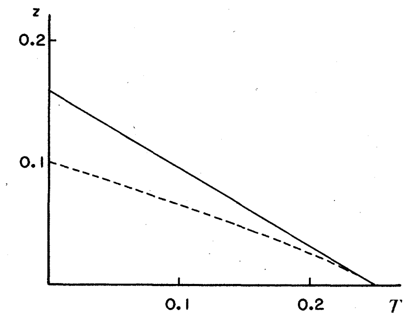

FIG. 1. Kosterlitz-Thouless phase-transition line in the (T,z) plane for a 2D Coulomb gas as obtained from the two lowest-order renormalization-group equations. Solid line: lowest-order RG equations [Eqs. (2.23)]. Dashed curve: Next-order RG equations [Eqs. (2.26)].

$$\frac{d}{dl}\frac{1}{T\tilde{\epsilon}(l)} = -\frac{2\pi z^2(l)}{T^2} + \frac{\pi^2}{T^2} z^2(l) \left[4 - \frac{1}{T\tilde{\epsilon}(l)}\right] , \tag{2.26a}$$

$$\frac{d}{dl} z(l) = \frac{z(l)}{2} \left[4 - \frac{1}{T\tilde{\epsilon}(l)}\right] + \frac{5}{4}\frac{\pi^2}{T^2} z^3(l) \; , \tag{2.26b}$$

which to leading order is integrated into (for $\epsilon_0 T < \frac{1}{4}$)

$$\left[\frac{1}{T} - 4\right]^2 + \frac{1}{2}\left[\frac{1}{T} - 4\right]^3 - \frac{\pi^2 z^2}{T^2}\left[4 + 5\left[\frac{1}{T} - 4\right]\right] = \left[\frac{1}{\epsilon_0 T} - 4\right]^2 + \frac{1}{2}\left[\frac{1}{\epsilon_0 T} - 4\right]^3 \tag{2.27}$$

giving the phase transition line

$$z = \frac{T}{\pi}\left[\frac{(1/T - 4)^2 + \frac{1}{2}(1/T - 4)^3}{4 + 5(1/T - 4)}\right]^{1/2} . \tag{2.28}$$

As an illustration Fig. 1 shows the phase line in the (T,z) plane as obtained from the two lowest-order RG approximations. In the following section we give a second prerequisite needed in the present approach: the sine-Gordon formulation.

III. SINE-GORDON FORMULATION

A thermal average for the CG may be turned into a functional integral over a real field.[17,18,10] The key identity in this connection is the following: Let the angular brackets $\langle \; \rangle_m$ denote

$$\langle O(\phi(\mathbf{r})) \rangle_m = \frac{\int d\phi \exp\left\{-\int d^2 r \left[\left[\frac{\nabla\phi}{2}\right]^2 + \frac{m^2}{2}\phi^2\right]\right\} O(\phi(\mathbf{r}))}{\int d\phi \exp\left\{-\int d^2 r \left[\left[\frac{\nabla\phi}{2}\right]^2 + \frac{m^2}{2}\phi^2\right]\right\}} , \tag{3.1}$$

where $\phi(\mathbf{r})$ is a real field, $\int d\phi$ denotes a functional integral over this field, and $O(\phi)$ denotes some functional of ϕ. Then one has the identity[17,18]

$$\left\langle \exp\left[-i\left[\frac{2\pi}{T}\right]^{1/2}\sum_i s_i\tilde{\phi}(\mathbf{r}_i)\right]\right\rangle_{m=0} = \exp\left[-\frac{1}{2T}\sum_{i,j}U(r_{ij})\right], \quad (3.2a)$$

where

$$\tilde{\phi}(\mathbf{r}) = \int d^2r' f_\xi(\mathbf{r}-\mathbf{r}')\phi(\mathbf{r}') . \quad (3.2b)$$

Using this identity the grand-partition function of the CG [Eq. (2.3)] may be expressed as[17,18]

$$Z = \left\langle \exp\left\{\int \frac{d^2r}{\xi^2} 2z\cos\left[\left[\frac{2\pi}{T}\right]^{1/2}\tilde{\phi}(\mathbf{r})\right]\right\}\right\rangle_{m=0} = \frac{\int d\phi \exp\left[-\int d^2r \mathscr{H}_{\text{sG}}(\mathbf{r})\right]}{\int d\phi \exp\left[-\int d^2r \frac{(\nabla\phi)^2}{2}\right]}, \quad (3.3a)$$

where $\mathscr{H}_{\text{sG}}$ is the Hamiltonian density for a nonlocal sine-Gordon theory:

$$\mathscr{H}_{\text{sG}}(\mathbf{r}) = \frac{(\nabla\phi)^2}{2} - \frac{2z}{\xi^2}\cos\left[\left[\frac{2\pi}{T}\right]^{1/2}\tilde{\phi}(\mathbf{r})\right] . \quad (3.3b)$$

We will in the following also make use of sine-Gordon angular brackets $\langle\ \rangle_{\text{sG}}$ which are defined by [in analogy with Eq. (3.1)]

$$\langle O(\phi(\mathbf{r}))\rangle_{\text{sG}} \equiv \frac{\int d\phi \exp\left[-\int d^2r \mathscr{H}_{\text{sG}}(\mathbf{r})\right] O(\phi(\mathbf{r}))}{\int d\phi \exp\left[-\int d^2r \mathscr{H}_{\text{sG}}(\mathbf{r})\right]} . \quad (3.4)$$

The one particle Green's function in the sine-Gordon theory $G(r)$ is given by

$$G(r) = \langle \phi(\mathbf{r})\phi(0)\rangle_{\text{sG}} . \quad (3.5)$$

We will in the following need the linearly screened potential $V_L(r)$ and the charge-density correlation function $\langle n(r)n(0)\rangle$ expressed as sine-Gordon correlation functions. They are given by[18] (the derivations are indicated in Appendix A)

$$V_L(r) = 2\pi G(r) . \quad (3.6)$$

The point-charge density is defined by

$$n^0(\mathbf{r}) = \sum_{i=1}^{N} s_i\delta(\mathbf{r}-\mathbf{r}_i) \quad (3.7)$$

for a configuration of N particles, and the point-charge-density correlation function is given by

$$\langle n^0(r)n^0(0)\rangle = -\frac{4z^2}{\xi^4}\left\langle \sin\left[\left[\frac{2\pi}{T}\right]^{1/2}\tilde{\phi}(\mathbf{r})\right]\sin\left[\left[\frac{2\pi}{T}\right]^{1/2}\tilde{\phi}(0)\right]\right\rangle_{\text{sG}} + \delta(\mathbf{r})\frac{2z}{\xi^2}\left\langle \cos\left[\left[\frac{2\pi}{T}\right]^{1/2}\tilde{\phi}(0)\right]\right\rangle_{\text{sG}} . \quad (3.8)$$

One notes that the point-charge-density correlation function is related to the CG—charge-density correlation function by convolutions

$$\langle n(\mathbf{r})n(0)\rangle = \int d^2r' d^2r'' f_\xi(\mathbf{r}-\mathbf{r}')f_\xi(\mathbf{r}'') \times \langle n^0(r')n^0(r'')\rangle . \quad (3.9)$$

As a check on the correctness and consistency of these expressions, in Appendix A we give an unusual derivation of the linear screening formula

$$V_L(k) = \frac{2\pi}{k^2}\left[1 - \frac{2\pi}{k^2T}\langle n(\mathbf{k})n(-\mathbf{k})\rangle\right] \quad (3.10)$$

entirely within the sine-Gordon formulation. Equation (3.10) will be important in the following.

IV. NEW RENORMALIZATION EQUATIONS

The basis for the new equations is straightforward in the sine-Gordon formulation. We make a cumulant expansion of the correlation

$$\left\langle \exp\left[i\left[\frac{2\pi}{T}\right]^{1/2}[\tilde{\phi}(\mathbf{r})\pm\tilde{\phi}(0)]\right]\right\rangle_{\text{sG}}$$

and keep only the lowest-order nonvanishing cumulant, i.e.,

$$\left\langle \exp\left[i\left[\frac{2\pi}{T}\right]^{1/2}[\tilde{\phi}(\mathbf{r})\pm\tilde{\phi}(0)]\right]\right\rangle_{\text{sG}} = \exp\left[-\frac{\pi}{T}\langle[\tilde{\phi}(\mathbf{r})\pm\tilde{\phi}(0)]^2\rangle_{\text{sG}}\right] . \quad (4.1)$$

Our faith in this approximation stems from the following reasons: It is the first term in a systematic expansion, it turns out to be connected to an appealing physical interpretation (given in the following section), and it leads to equations which compare favorably with lowest-order RG equations [Eqs. (2.23) and (2.26); compare Sec. VI].

Applying Eq. (4.1) to the correlation, Eq. (3.8), gives

$$\left\langle \sin\left[\left(\frac{2\pi}{T}\right)^{1/2}\tilde{\phi}(\mathbf{r})\right]\sin\left[\left(\frac{2\pi}{T}\right)^{1/2}\tilde{\phi}(0)\right]\right\rangle_{\rm sG}=\tfrac{1}{2}\mathrm{Re}\left\langle \exp\left[i\left(\frac{2\pi}{T}\right)^{1/2}[\tilde{\phi}(\mathbf{r})-\tilde{\phi}(0)]\right]-\exp\left[i\left(\frac{2\pi}{T}\right)^{1/2}[\tilde{\phi}(\mathbf{r})+\tilde{\phi}(0)]\right]\right\rangle_{\rm sG}$$

$$=\tfrac{1}{2}\exp\left[-\frac{\pi}{T}\langle[\tilde{\phi}(\mathbf{r})-\tilde{\phi}(0)]^2\rangle_{\rm sG}\right]\left[1-\exp\left[-\frac{4\pi}{T}\langle\tilde{\phi}(\mathbf{r})\tilde{\phi}(0)\rangle_{\rm sG}\right]\right]. \quad (4.2)$$

Using Eqs. (3.5) and (3.6) we may express this in the linearly screened potential as

$$\left\langle \sin\left[\left(\frac{2\pi}{T}\right)^{1/2}\tilde{\phi}(\mathbf{r})\right]\sin\left[\left(\frac{2\pi}{T}\right)^{1/2}\tilde{\phi}(0)\right]\right\rangle_{\rm sG}=\tfrac{1}{2}\exp\left[\frac{1}{T}[\tilde{V}_L(r)-\tilde{V}_L(0)]\right]\left[1-\exp\left[-\frac{2}{T}\tilde{V}_L(r)\right]\right], \quad (4.3a)$$

where

$$\tilde{V}_L(r)=\int d^2r' d^2r'' f_\xi(\mathbf{r}-\mathbf{r}')V_L(|\mathbf{r}'-\mathbf{r}''|)f_\xi(\mathbf{r}''). \quad (4.3b)$$

We will in the following only deal with the low-temperature phase where the screening length λ is infinite. To leading order in λ/ξ one has[10]

$$V_L(r)\sim\ln(\lambda/\xi). \quad (4.4)$$

Consequently, in the low-temperature phase Eq. (4.3a) simplifies to

$$\left\langle \sin\left[\left(\frac{2\pi}{T}\right)^{1/2}\tilde{\phi}(\mathbf{r})\right]\sin\left[\left(\frac{2\pi}{T}\right)^{1/2}\tilde{\phi}(0)\right]\right\rangle_{\rm sG}=\tfrac{1}{2}\exp\left[\frac{1}{T}[\tilde{V}_L(r)-\tilde{V}_L(0)]\right]. \quad (4.5)$$

For $r>\xi$ one may ignore the difference between $\langle n(r)n(0)\rangle$ and the point-charge-density correlation $\langle n^0(r)n^0(0)\rangle$. Combining Eqs. (3.8) and (4.5) then gives

$$\langle n(r)n(0)\rangle=-\frac{2z^2}{\xi^4}\exp\left[\frac{1}{T}[\tilde{V}_L(r)-\tilde{V}_L(0)]\right]. \quad (4.6)$$

Equation (4.6) together with the linear screening expression Eq. (3.10), constitute a self-consistent set of equations. This set of equations is the basis for the present paper.

The self-consistent character is brought out more explicitly by expressing $\tilde{V}_L(r)-\tilde{V}(0)$ as

$$\tilde{V}_L(\mathbf{r})-\tilde{V}(0)=\int_0^r\frac{\partial\tilde{V}_L(r)}{\partial r}dr\approx\int_\xi^r\frac{\partial V_L(r)}{\partial r}dr$$

$$=-\int_\xi^r F(r)\,dr, \quad (4.7)$$

where F, the force between two infinitesimal test charges of opposite sign, is given in Eqs. (2.19). The point is that F may be explicitly expressed in terms of $\langle n(r)n(0)\rangle$ which turns Eq. (4.6) into a self-consistent equation for $\langle n(r)n(0)\rangle$. The derivation is given in Appendix B. In Eq. (4.7) we have also made some minor simplifications; the CG test charges are replaced by point test charges so that $\tilde{V}_L(r)$ is replaced by $V_L(r)$, which is valid for $r>\xi$ (see Ref. 13); in addition we used $\tilde{V}_L(\xi)-\tilde{V}_L(0)\approx 0$ (see Ref. 13) so that the lower integration limit may be replaced by ξ.

In order to make a connection with the RG equations [Eqs. (2.23) and (2.26)] we introduce a logarithmic length scale $l=\ln(r/\xi)$ and a renormalized fugacity $z(l)$

$$z(l)=\exp\left[2l-\frac{1}{2T}\int_\xi^r F(r)\,dr\right]. \quad (4.8)$$

Equations (4.6) and (4.7) may then be expressed in differential form as

$$\frac{d}{dl}\frac{1}{T\tilde{\epsilon}(l)}=-\frac{2z^2(l)\pi^2}{T^2}, \quad (4.9a)$$

$$\frac{d}{dl}z(l)=\frac{z(l)}{2}\left[4-\int_0^\infty dx e^{-x}x\frac{1}{T\tilde{\epsilon}(l+x/2)}\right], \quad (4.9b)$$

where $\tilde{\epsilon}(l)$ is the length-dependent dielectric function introduced in Eq. (2.18), expressed here as a function of the logarithmic length scale l. The initial conditions are $z(l=0)=z$ and $\tilde{\epsilon}(l=0)=1$. The key quantity $\epsilon_0=\tilde{\epsilon}(\infty)$ may be obtained by integration (see Sec. VI). The algebra leading to Eqs. (4.9) is given in Appendix B. Equations (4.9) are our new renormalization equations.

The last term on the right-hand side of Eq. (4.9b) may, by partial integration, be expressed as

$$\int_0^\infty dx\,e^{-x}x\frac{1}{T\tilde{\epsilon}(l+x/2)}=\sum_{n=0}^\infty\frac{n+1}{2^n}\frac{d^n}{dl^n}\frac{1}{T\tilde{\epsilon}(l)}, \quad (4.10)$$

which inserted in Eqs. (4.9) gives

$$\frac{d}{dl}z(l)=\frac{z(l)}{2}\left[4-\frac{1}{T\tilde{\epsilon}(l)}\right]+O(z^3(l)). \quad (4.11)$$

One notes that the lowest-order RG equations [Eqs. (2.23)] are regained as the lowest-order approximation of the new renormalization equations [Eqs. (4.9)]. In the following section we give an interpretation for the physical origin of the higher-order terms of the new renormalization equations.

V. LENGTH-DEPENDENT SCREENING

Figure 2 shows two (2D) test particles of opposite charge separated by a distance r_0 with the origin at the center of the test pair. The (2D) electrical field $D(\mathbf{r})$ caused by the test pair in the absence of surrounding CG charges is given by

$$\mathbf{D}(\mathbf{r})=\mathbf{D}_1(\mathbf{r})+\mathbf{D}_2(\mathbf{r})=\frac{\mathbf{r}-\mathbf{r}_0/2}{(\mathbf{r}-\mathbf{r}_0/2)^2}-\frac{\mathbf{r}+\mathbf{r}_0/2}{(\mathbf{r}+\mathbf{r}_0/2)^2}\ . \tag{5.1}$$

The interaction energy between the test particles in the absence of the CG charges is then

$$\begin{aligned}U_0(r_0)&=\frac{1}{4\pi}\int d^2r 2\mathbf{D}_1(\mathbf{r})\cdot\mathbf{D}_2(\mathbf{r})\\&=-\int_0^\infty dr\int_0^{2\pi}\frac{d\phi}{2\pi}\frac{r(r^2-r_0^2/4)}{(r^2-rr_0\cos\phi+r_0^2/4)(r^2+rr_0\cos\phi+r_0^2/4)}=-\int_0^\infty dr\frac{r}{r^2+r_0^2/4}\operatorname{sgn}(r-r_0/2)\end{aligned} \tag{5.2}$$

(for the last equality see Ref. 19). Let us now introduce a length-dependent dielectric function $\tilde{\epsilon}(r)$ which takes into account the polarization of the test-particle interaction due to CG dipoles with a separation less than r. The intuitive length-dependent screening idea may be stated as follows: The electric field D taken on a circle of diameter d centered at the origin is effectively polarized only by CG dipoles with a separation smaller than d. Following this intuitive argument one obtains for the interaction energy between the test particles

$$U_1(r_0)=\frac{1}{4\pi}\int d^2r\frac{2\mathbf{D}_1(\mathbf{r})\cdot\mathbf{D}_2(\mathbf{r})}{\tilde{\epsilon}(2r)}\ , \tag{5.3}$$

which, using Eq. (5.2), becomes

$$\begin{aligned}U_1(r_0)=&\int_0^{r_0/2}dr\frac{r}{r^2+r_0^2/4}\frac{1}{\tilde{\epsilon}(2r)}\\&-\int_{r_0/2}^\infty dr\frac{r}{r^2+r_0^2/4}\frac{1}{\tilde{\epsilon}(2r)}\ .\end{aligned} \tag{5.4}$$

The force F acting between the test particles,

$$F=\frac{d}{dr_0}U_1(r_0)\ ,$$

is then

$$\begin{aligned}F=&\frac{1}{r_0}\frac{1}{\epsilon(r_0)}+\int_0^{r_0/2}dr\frac{d}{dr_0}\left[\frac{r}{r^2+r_0^2/4}\right]\frac{1}{\tilde{\epsilon}(2r)}\\&-\int_{r_0/2}^\infty dr\frac{d}{dr_0}\left[\frac{r}{r^2+r_0^2/4}\right]\frac{1}{\tilde{\epsilon}(2r)}\ .\end{aligned} \tag{5.5}$$

By partial integration and change of variable this becomes

$$\begin{aligned}F=&\frac{1}{r_0\tilde{\epsilon}(r_0)}+\frac{1}{r_0}\left[\frac{1}{\tilde{\epsilon}(r_0)}-1\right]\\&-r_0\int_0^{r_0}dr\frac{1}{r_0^2+r^2}\frac{d}{dr}\frac{1}{\tilde{\epsilon}(r)}\\&+r_0\int_{r_0}^\infty dr\frac{1}{r^2+r_0^2}\frac{d}{dr}\frac{1}{\tilde{\epsilon}(r)}\ .\end{aligned} \tag{5.6}$$

Now we use the approximation

$$\frac{1}{r^2+r_0^2}\approx\begin{cases}\dfrac{1}{r^2} & \text{for } r>r_0\\ 1/r_0^2 & \text{for } r_0>r\end{cases}$$

and Eq. (5.6) reduces to

$$F=\frac{1}{r_0\tilde{\epsilon}(r_0)}+r_0\int_{r_0}^\infty dr\frac{1}{r^2}\frac{d}{dr}\frac{1}{\tilde{\epsilon}(r)}\ . \tag{5.7}$$

By inserting the expression given in Eq. (2.18) for $\tilde{\epsilon}(r)$ this results in

$$F=\frac{1}{r_0\tilde{\epsilon}(r_0)}+\frac{\pi^2r_0}{T}\int_{r_0}^\infty dr\, r\langle n(r)n(0)\rangle\ . \tag{5.8}$$

The point is that we have rederived the two first contributions to F in Eqs. (2.19) from the length-dependent screening idea. As a consequence, these two contributions may be given the following physical interpretation: The first term is caused by the electric field between the test particles polarized by CG dipoles which have smaller separation than the test pair. The second term is caused by the dipole field outside the test pair polarized by CG dipoles which have larger separation than the test pair.

The remaining contribution F_3 [see Eqs. (2.19)] may also be tied to an intuitive physical interpretation: The polarizability of the test pair is given by

$$\alpha(r_0)=\frac{r_0^2}{2T}\ . \tag{5.9}$$

The dipole energy of the test pair is given by

$$U_{\text{test}}=-\tfrac{1}{2}\alpha(r_0)D^2\ , \tag{5.10}$$

where D^2 is the average of the square of the electric field

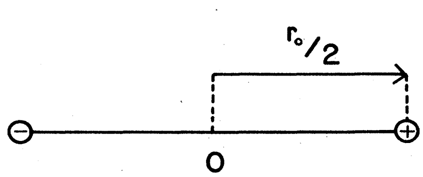

FIG. 2. The test dipole pair. The test particles have opposite charge, are symmetrically placed with respect to the origin, and are separated by the vector $\mathbf{r}_0$.

caused by the CG particles. The total energy of the CG in the absence of the test pair is given by

$$U_{\rm tot}=\frac{\Omega}{4\pi}D^2\ , \tag{5.11}$$

which may also be expressed as

$$U_{\rm tot}=\frac{\Omega}{2}\int d^2r U(r)\langle n(r)n(0)\rangle\ . \tag{5.12}$$

Now since $U(r)\approx -\ln(r/\xi)+\text{const}$ and $\int d^2r\langle n(r)n(0)\rangle=0$ by the charge-neutrality condition, we obtain from Eqs. (5.9)–(5.12) that

$$\frac{dU_{\rm test}}{dr_0}=\frac{2\pi^2 r_0}{T}\int_0^\infty dr\, r\ln(r/r_0)\langle n(r)n(0)\rangle\ . \tag{5.13}$$

One notes that $dU_{\rm test}/dr_0$ is equal to F_3 of Eqs. (2.19) except that the lower integration limit is 0 instead of r_0. However, this difference is also intuitively understandable; only CG dipoles with separations larger than the test pair contribute to the average electric field felt by the test pair.

The point with the physical reasoning in the present section is the following: In the preceding section we derived new renormalization equations [Eqs. (4.9)] from the first term of a cumulant expansion. We can now give a heuristic derivation of the same equations by improving the arguments leading to the lowest-order RG equations [Eqs. (2.23)]. The only difference is the estimate of the force F acting between the particles in a dipole which gives rise to the change

$$U_{\rm dip}(r)=\int_\xi^r dr' F(r)\ , \tag{5.14}$$

where F is given by Eqs. (2.19) instead of Eq. (2.20). The reason for this new estimate is that the force between the particles of a dipole is affected *both* by smaller and larger dipoles. The larger dipoles polarize the dipole field surrounding the dipole pair considered, and provide an electric field in which the dipole pair considered orients. From this viewpoint the difference between the lowest-order RG equations [Eqs. (2.23)] and the new renormalization equations [Eqs. (4.9)] is the inclusion of the effect of the larger dipoles.

VI. NUMERICAL SOLUTION

The solution of Eqs. (4.9) may be obtained by numerical integration. For this purpose we found it convenient to rewrite Eqs. (4.9) as (see Appendix C)

$$h(l)=h(0)\exp\left[\left[4-\frac{1}{\tilde\epsilon(0)T}-C_0(l)\right]l - C_0(l)+C_1(l)-C_2(l)\right]\ , \tag{6.1a}$$

$$C_0(l)=\int_0^l dx\, h(x)\ , \tag{6.1b}$$

$$C_1(l)=\int_0^l dx\, xh(x)\ , \tag{6.1c}$$

$$C_2(l)=\tfrac{1}{4}\int_0^\infty dx(x+2)e^{-x}[h(l+x/2)-h(x/2)]\ , \tag{6.1d}$$

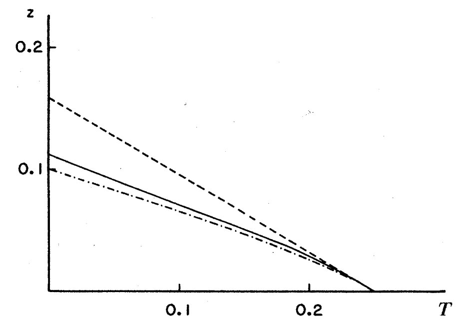

FIG. 3. Kosterlitz-Thouless phase-transition line in the (T,z) plane as obtained from the new renormalization equations [Eqs. (4.9) and (6.1)]. Solid curve: new equations; dashed line: lowest-order RG equations [Eqs. (2.23)]; dashed-dotted curve: next-order RG equations [Eqs. (2.26)].

with the boundary conditions $h(0)=-2\pi^2z^2/T^2$, $h(\infty)=0$, and $\tilde\epsilon(0)=1$. Equations (6.1) may be solved by numerical iteration, e.g., starting from

$$h_{\rm start}(l)=h(0)\exp[(4-1/T)l]\ .$$

The key quantity ϵ_0 is obtained as

$$\epsilon_0=\left[1+T\int_0^\infty dx\, h(x)\right]^{-1}\ . \tag{6.2}$$

Figure 3 shows the critical line in the (T,z) plane as obtained from Eqs. (6.1) (solid curve). It is compared to the result from the lowest-order RG equations [Eqs. (2.23)] (dashed line) and to the next-order RG equations [Eqs. (2.26)] (dashed-dotted curve). One notes that the critical line from Eqs. (6.1) comes close to the result from the next-order RG equations [Eqs. (2.26)]. This indicates that the new equations are indeed an improvement of the lowest-order RG equations [Eqs. (2.23)] as we expected. In this comparison it should be noted that the lowest-order RG equations [Eqs. (2.23)] are by construction valid close to $z=0$, the next-order equations [Eqs. (2.26)] close to $z=0$, and $T-\frac{1}{4}=0$, whereas the effective expansion parameter in the cumulant expansion leading to Eqs. (4.9) is unknown at present. However, we believe that the cu-

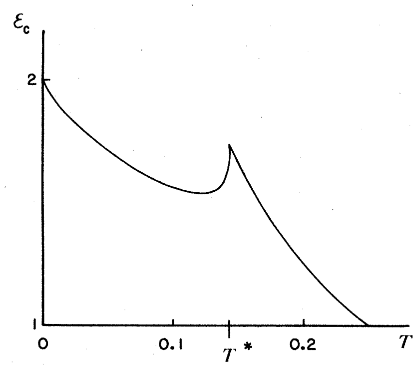

FIG. 4. Value of the dielectric constant at the phase transition, ϵ_c, as a function of temperature T. The function $\epsilon_c(T)$ has a cusp at the temperature T^*.

mulant expansion is less restrictive.

Figure 4 shows ϵ_c (the value of ϵ_0 at the critical line) as a function of temperature. This quantity has a cusp at a temperature T^* (≈ 0.1436). As the critical temperature approaches T^* from below, ϵ_c behaves as

$$\epsilon_c(T_c)=\frac{1}{4T^*}-\text{const}\times(T^*-T_c)^{1/2} . \tag{6.3}$$

This is demonstrated in Fig. 5, where $(\epsilon_c-1/4T^*)^2$ is plotted as a function of T_c (solid curve). The solid curve falls on the dashed line in the figure as T^* is approached, in agreement with Eq. (6.3). Above T^* the quantity ϵ_c is equal to $1/4T_c$. This result is in agreement with the RG equations[8,16] [Eqs. (2.23) and (2.26)]. Below T^* Eqs. (6.1) give $\epsilon_c<1/4T_c$ (compare Fig. 4). This result is not contained in the lowest-orders RG equations[8,16] [Eqs. (2.23) and (2.26)]. However, it is compatible with these equations since the critical properties derived from them involve the restriction $|T_c-\frac{1}{4}|\ll 1$. As T approaches T_c from below for constant z the quantity ϵ_0 obtained from Eqs. (6.1) behaves as

$$\epsilon_0(T)=\epsilon_c-\text{const}\times(T_c-T)^{1/2} . \tag{6.4}$$

This behavior is demonstrated in Fig. 6. Figure 6(a) is a case when $T_c>T^*$. We use the fact that $\epsilon_c=1/4T_c$ and plot $(\epsilon_0-1/4T)^2$ as a function of T (solid curve). The solid curve in the figure approaches the dashed line as T comes close to the critical temperature T_c, in agreement with Eq. (6.4). Figure 6(b) is a case when $T_c<T^*$, $(\epsilon_0-\epsilon_c)^2$ is plotted as a function of T (solid curve). As in Fig. 6(a) the solid curve approaches the dashed line as T comes close to T_c. The constant in Eq. (6.4) diverges logarithmically at T^*. This is demonstrated in Fig. 7. We rewrite Eq. (6.4) as

$$\epsilon_0(T)=\epsilon_c-A_{+(-)}(T_c)(T_c-T)^{1/2} , \tag{6.5}$$

where $A_{+(-)}$ refers to $T_c>T^*$ ($T_c<T^*$). The constants A_+ and A_- are plotted as functions of $X=-\ln(|T_c-T^*|)$. As T_c approaches T^*, X becomes large, and both A_+ and A_- turn into straight lines as

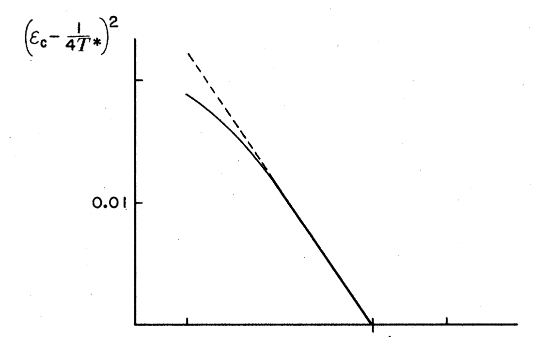

FIG. 5. As the temperature T^* is approached from below, the function $\epsilon_c(T)$ behaves as $\epsilon_c(T)=1/4T^*-\text{const}\times(T^*-T)^{1/2}$. This is illustrated by plotting $(\epsilon_c-1/4T^*)^2$ as a function of T. Solid curve: $(\epsilon_c-1/4T^*)^2$; dashed line: tangent of solid curve at T^*.

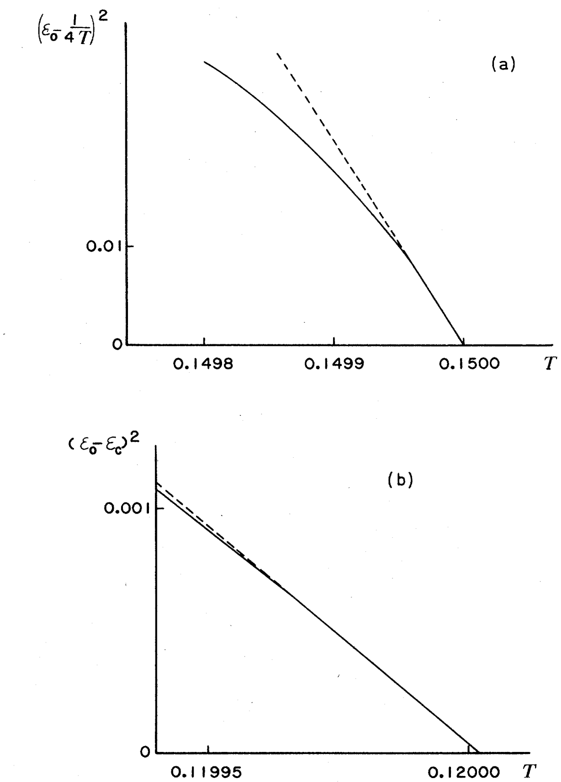

FIG. 6. As the critical line is approached from below for constant z, the function $\epsilon_0(T)$ behaves as $\epsilon_0(T)=\epsilon_c(T_c)-\text{const}\times(T_c-T)^{1/2}$. Panel (a) is a case when $T_c>T^*$. In this case $\epsilon_c(T_c)=1/4T_c$ and we have plotted $(\epsilon_0-1/4T)^2$ as a function of T. Solid curve: $(\epsilon_0-1/4T)^2$; dashed line: tangent of solid curve at T_c. Panel (b) is a case where $T_c<T^*$. In this case $\epsilon_c\neq 1/4T_c$ and we have plotted $(\epsilon_0-\epsilon_0)^2$ as a function of T. Solid curve: $(\epsilon_0-\epsilon_c)^2$; dashed line: tangent of solid curve at T_c.

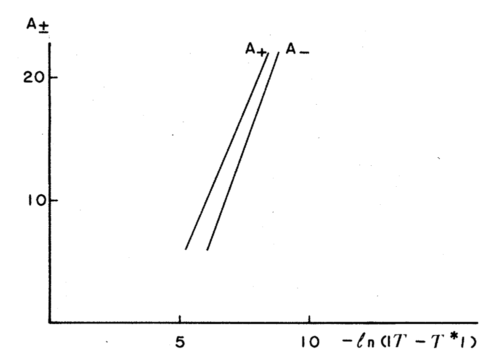

FIG. 7. As the critical line is approached from below for constant z, the function $\epsilon_0(T)$ behaves as $\epsilon_0(T)=\epsilon_c(T_c)-A_{+(-)}(T_c-T)^{1/2}$ where $A_{+(-)}$ refers to $T_c>T^*$ ($T_c<T^*$). $A_{+(-)}$ diverges logarithmically as T_c approaches T^*. This is illustrated by plotting $A_{+(-)}$ as functions of $-\ln(|T_c-T^*|)$. The figure shows that both A_+ and A_- are within numerical accuracy straight lines for a large enough abscissa.

seen in Fig. 7. We note that a slight adjustment of T^* (i.e., $T^* \approx 0.143\,56$) would make the two lines in Fig. 7 parallel. However, our estimated numerical accuracy for T^* is only about $T^*=0.1436\pm 5\times 10^{-5}$. In the following section we discuss some implications of the numerical solutions described in the present section.

VII. CONCLUSIONS

A striking feature of the solution to the new renormalization equations [Eqs. (4.9)] is the appearance of a new temperature T^*. This temperature is related to the structure of the RG flow diagram. The RG trajectories are trajectories with constant $T\epsilon_0$, where $T\epsilon_0$ is regarded as a function of $T\tilde{\epsilon}(l)$ and $z(l)/T$. The RG flow diagram corresponding to Eqs. (4.9) is given in Fig. 8. The critical line between $T_c=\frac{1}{4}$ and $T_c=T^*$ is given by the RG trajectory $T\epsilon_0=\frac{1}{4}$. Between $T_c=T^*$ and $T_c=0$, the critical line is the loci of starting points for the RG trajectories (dashed curve in Fig. 8). The RG trajectories in Fig. 8 (solid curves with arrows) correspond from right to left to $T\epsilon_0=\frac{1}{4}$, $\frac{1}{6}$, and $\frac{1}{12}$, respectively.

Above the critical line ϵ_0 is infinite. At the critical line ϵ_0 jumps from ϵ_c to infinity. This means that the quantity $1/T\epsilon_0$ jumps from 4 to 0 at the critical line in the interval $T^*\leq T\leq\frac{1}{4}$ since the critical line is given by $T\epsilon_c=\frac{1}{4}$ in this interval. This is the universal jump[6] expressed in the CG language.[10] The new feature is that this prediction only holds for $T_c>T^*$. Below T^* the jump in $1/T\epsilon_0$ at the critical line is larger and *nonuniversal.* The size of the jump as obtained from Eqs. (4.9) is given in Fig. 9.

The question whether a particular system has a universal or a nonuniversal jump at its Kosterlitz-Thouless transition consequently depends on whether the CG temperature corresponding to the transition is larger or smaller than T^*. This is discussed further in a separate paper in connection with half-frustrated XY models, where empirical evidence in favor of a nonuniversal jump was found.[9]

The quantity $T\epsilon_0$ also turns up in connection with critical indices, e.g., from Eq. (4.6) we have

$$\langle n(r)n(0)\rangle \sim \exp\left[\frac{1}{T}[\tilde{V}_L(r)-\tilde{V}_L(0)]\right]. \tag{7.1}$$

For large r the leading behavior of $\tilde{V}_L(r)-\tilde{V}_L(0)$ is $(1/\epsilon_0)\ln(\xi/r)$ below the critical line [compare Eqs. (2.9)] so that

$$\langle n(r)n(0)\rangle \sim \left[\frac{\xi}{r}\right]^{1/T\epsilon_0} \quad \text{for } r\to\infty\ . \tag{7.2}$$

It is likewise possible to show that the leading behavior for the spin-spin correlations of the XY models below the critical line is $\sim(1/r)^{\eta}$ for large r, where η is given by $\eta=T\epsilon_0$.[14] Thus, for example, the critical index η has the universal value $\frac{1}{4}$ at the critical line in the CG temperature interval $T^*<T<\frac{1}{4}$, whereas it is nonuniversal and smaller than $\frac{1}{4}$ in the interval $0\leq T<T^*$.

In recapitulation, we have presented a new set of renormalization equations for the Kosterlitz-Thouless transition. These equations were motivated both from a cumulant expansion of a field-theoretic formulation, and more physically, from the point of view of length-dependent screening in a Coulomb gas. These equations single out a new special temperature T^*. This temperature is reflected in the structure of the RG flow diagram. The RG flow structure leads to nonuniversal behavior at the critical line below T^* like $\eta<\frac{1}{4}$ and a nonuniversal jump.

It should be noted that the cumulant expansion used to derive the new equations involve an unknown expansion parameter. Hence nothing is known at present about the influence of the higher-order cumulants on the results presented here. On the other hand, the physical motivation of the equations in terms of length-dependent screen-

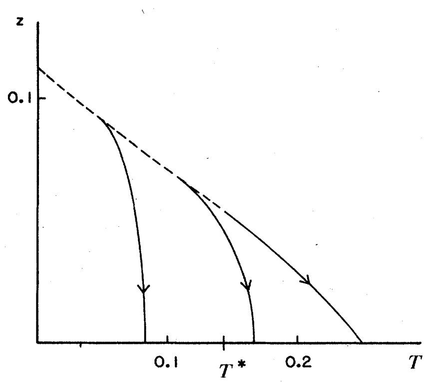

FIG. 8. Structure of the renormalization flow diagram corresponding to the new renormalization equations [Eqs. (4.9) and (6.1)]. Solid curves with arrows: trajectories with constant $T\epsilon_0$. From right to left the trajectories are $T\epsilon_0=\frac{1}{4}$, $\frac{1}{6}$, and $\frac{1}{12}$, respectively. Dashed curve: The loci of starting points for trajectories with constant $T\epsilon_0$. The trajectory $T\epsilon_0=\frac{1}{4}$ starts at T^* and is the critical line for $T^*\leq T_c\leq\frac{1}{4}$. For $T_c<T^*$ the critical line is given by the loci of starting points (dashed curve).

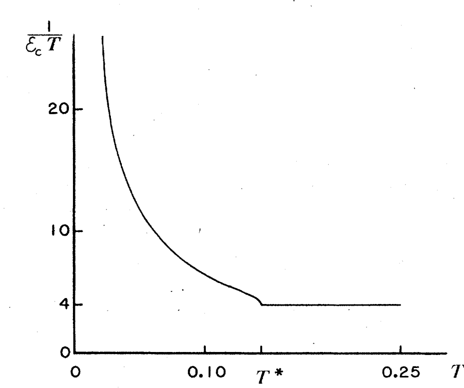

FIG. 9. Size of the jump as obtained from the new renormalization equations [Eqs. (4.9) and (6.1)]. In the interval $T^*<T<\frac{1}{4}$ the value is given by the universal jump prediction $1/\epsilon_c T=4$. Below T^* the value of the jump is larger and nonuniversal.

ing suggests to us that they are physically sound.

It should also be noted that the new equations complement the low-order RG equations in the sense that the low-order RG equations are derived within a restricted part of a two-dimensional parameter space, whereas the new equations represent an attempt to find approximate equations applying to a larger part of the parameter space.[20]

ACKNOWLEDGMENT

This work was supported by Swedish Natural Science Research Council Grant No. 4040-101.

APPENDIX A

In analogy with Eqs. (3.3) we use the identity Eqs. (3.2) to rewrite the total grand-partition function, Z_{tot}, which includes two point test charges with opposite infinitesimal charge, δ_s, one at the origin and one at $\mathbf{r}$. The total free energy then becomes

$$F=-T\ln(Z_{\text{tot}})$$
$$=-T\ln\left\langle \exp\left\{\int \frac{d^2r'}{\xi^2}2z\cos\left[\left[\frac{2\pi}{T}\right]^{1/2}\tilde{\phi}(\mathbf{r}')\right]\right\} \times\exp\left[-i\delta s\left[\frac{2\pi}{T}\right]^{1/2}[\phi(\mathbf{r})-\phi(0)]\right]\right\rangle_{\text{sG}} . \quad \text{(A1)}$$

It follows that the part of the free energy which is proportional to $(\delta s)^2$ is given by

$$\frac{1}{2}\frac{\partial^2}{\partial(\delta s)^2}F\bigg|_{\delta s=0}=\frac{2\pi}{2}\langle[\phi(\mathbf{r})-\phi(0)]^2\rangle_{\text{sG}}$$
$$=-2\pi\langle\phi(\mathbf{r})\phi(0)\rangle_{\text{sG}}+2\pi\langle\phi(0)^2\rangle_{\text{sG}} . \quad \text{(A2)}$$

From the definition of the linearly screened potential, $V_L(r)$, (given in Sec. II) it follows that

$$V_L(0)-V_L(r)=-2\pi G(r)+2\pi G(0) , \quad \text{(A3)}$$

and hence

$$V_L(r)=2\pi G(r)+\text{const} . \quad \text{(A4)}$$

The constant on the right-hand side is 0, as is found by performing the functional integral for $G(r)$ in the case $z=0$, and Eq. (3.6) follows.

Equation (3.8) may also be deduced by use of Eqs. (3.2): Start with the point-charge density for a CG configuration with N particles

$$n^0(\mathbf{r})=\sum_{i=1}^{N}s_i\delta(\mathbf{r}-\mathbf{r}_i) .$$

It follows that

$$\langle n^0(r)n^0(0)\rangle\,|_N\sim\sum_{kl}s_ks_l\left[\left[\frac{N}{2}\right]!\right]^{-2}z^N\prod_{i=1}^{N}\int\frac{d^2r_i}{\xi^2}\exp\left[-\frac{1}{2T}\sum_{i,j}s_is_jU_{ij}(r_{ij})\right]\delta(\mathbf{r}-\mathbf{r}_k)\delta(\mathbf{r}_l)$$
$$=\sum_{kl}s_ks_l\left[\left[\frac{N}{2}\right]!\right]^{-2}z^N\prod_{i}^{N}\int\frac{d^2r_i}{\xi^2}\left\langle\exp\left[-i\left[\frac{2\pi}{T}\right]^{1/2}\sum s_i\tilde{\phi}(\mathbf{r}_j)\right]\right\rangle_{m=0}\delta(\mathbf{r}-\mathbf{r}_k)\delta(\mathbf{r}_l)$$
$$=\left[\frac{N}{2}\right]^2\left[\left[\frac{N}{2}\right]!\right]^{-2}\frac{z^N}{\xi^4}\left\{\left\langle\exp\left[-i\left[\frac{2\pi}{T}\right]^{1/2}[\tilde{\phi}(\mathbf{r})+\tilde{\phi}(0)]\right]\right\rangle_{m=0}+\left\langle\exp\left[i\left[\frac{2\pi}{T}\right]^{1/2}[\tilde{\phi}(\mathbf{r})+\tilde{\phi}(0)]\right]\right\rangle_{m=0}\right.$$
$$-\left\langle\exp\left[i\left[\frac{2\pi}{T}\right]^{1/2}[\tilde{\phi}(\mathbf{r})-\tilde{\phi}(0)]\right]\right\rangle_{m=0}$$
$$\left.-\left\langle\exp\left[-i\left[\frac{2\pi}{T}\right]^{1/2}[\tilde{\phi}(\mathbf{r})-\tilde{\phi}(0)]\right]\right\rangle_{m=0}\right\}$$
$$\times\prod_{i=1}^{N-2}\int\frac{d^2r_i}{\xi^2}\left\langle\exp\left[-i\left[\frac{2\pi}{T}\right]^{1/2}\sum_j s_j\tilde{\phi}(\mathbf{r}_j)\right]\right\rangle_{m=0}$$
$$+\delta(\mathbf{r})\frac{z^N}{\xi^2}\frac{N}{2}\left[\left[\frac{N}{2}\right]!\right]^{-2}\left\{\left\langle\exp\left[-i\left[\frac{2\pi}{T}\right]^{1/2}\tilde{\phi}(0)\right]\right\rangle_{m=0}+\left\langle\exp\left[i\left[\frac{2\pi}{T}\right]^{1/2}\tilde{\phi}(0)\right]\right\rangle_{m=0}\right\}$$
$$\times\prod_{i=1}^{N-1}\frac{d^2r_i}{\xi^2}\left\langle\exp\left[-i\left[\frac{2\pi}{T}\right]^{1/2}\sum_j s_j\tilde{\phi}(\mathbf{r}_j)\right]\right\rangle_{m=0} . \quad \text{(A5)}$$

Summing all configurations with different N gives

$$\langle n^0(r)n^0(0)\rangle=-\frac{4z^2}{\xi^4}\left\langle\sin\left[\left[\frac{2\pi}{T}\right]^{1/2}\tilde{\phi}(\mathbf{r})\right]\sin\left[\left[\frac{2\pi}{T}\right]^{1/2}\tilde{\phi}(0)\right]\right\rangle_{\mathrm{sG}}+\delta(\mathbf{r})\frac{z}{\xi^2}\left\langle\cos\left[\left[\frac{2\pi}{T}\right]^{1/2}\tilde{\phi}(0)\right]\right\rangle_{\mathrm{sG}}. \tag{A6}$$

A derivation of linear screening *within* the sine-Gordon formulation goes as follows: Define an auxiliary function $Z_{\alpha\beta}$ by

$$Z_{\alpha\beta}\equiv\left\langle\exp\left[\int d^2r\mathscr{H}_{\alpha\beta}(r)\right]\right\rangle_{m=0} \tag{A7a}$$

with

$$\mathscr{H}_{\alpha\beta}(r)=\frac{2z}{\xi^2}\cos\left[\left[\frac{2\pi}{T}\right]^{1/2}\phi(r)+\alpha f_\xi(-\mathbf{k})e^{-i\mathbf{k}\cdot\mathbf{r}}+\beta f_\xi(\mathbf{k})e^{i\mathbf{k}\cdot\mathbf{r}}\right], \tag{A7b}$$

where $f_\xi(\mathbf{k})=\int d^2rf_\xi(\mathbf{r})e^{-i\mathbf{k}\cdot\mathbf{r}}$ is the Fourier transform of the single-particle charge distribution. It follows that

$$\begin{aligned}\frac{1}{\Omega}\frac{\partial}{\partial\alpha}\frac{\partial}{\partial\beta}\ln(Z_{\alpha\beta})\bigg|_{\alpha=\beta=0}&=\frac{1}{\Omega}\int d^2rd^2r'f_\xi(-\mathbf{k})f_\xi(\mathbf{k})e^{-i\mathbf{k}\cdot(\mathbf{r}-\mathbf{r}')}\frac{4z^2}{\xi^4}\left\langle\sin\left[\left[\frac{2\pi}{T}\right]^{1/2}\tilde{\phi}(\mathbf{r})\right]\sin\left[\left[\frac{2\pi}{T}\right]^{1/2}\tilde{\phi}(\mathbf{r}')\right]\right\rangle_{\mathrm{sG}}\\&\quad-\frac{2z}{\xi^2}f_\xi(\mathbf{k})f_\xi(-\mathbf{k})\left\langle\cos\left[\left[\frac{2\pi}{T}\right]^{1/2}\tilde{\phi}(0)\right]\right\rangle_{\mathrm{sG}}=-f_\xi(\mathbf{k})f_\xi(-\mathbf{k})\langle n^0(\mathbf{k})n^0(-\mathbf{k})\rangle=-\langle n(\mathbf{k})n(-\mathbf{k})\rangle\,.\end{aligned} \tag{A8}$$

In deriving Eq. (A8) we have dropped a term proportional to $[\langle\sin(2\pi/T)\tilde{\phi}(\mathbf{r})\rangle_{\mathrm{sG}}]^2$ since $\langle\sin(2\pi/T)\tilde{\phi}(\mathbf{r})\rangle_{\mathrm{sG}}=0$ which follows because it is an odd function of $\phi(\mathbf{r})$. Now make the transformation

$$\phi'(\mathbf{r})=\phi(\mathbf{r})+\left[\frac{T}{2\pi}\right]^{1/2}\alpha e^{-i\mathbf{k}\cdot\mathbf{r}}+\left[\frac{T}{2\pi}\right]^{1/2}\beta e^{i\mathbf{k}\cdot\mathbf{r}}, \tag{A9}$$

which gives

$$\mathscr{H}'_{\alpha\beta}(\mathbf{r})=-\left[\left[\frac{T}{2\pi}\right]^{1/2}i\mathbf{k}e^{-i\mathbf{k}\cdot\mathbf{r}}\alpha-\left[\frac{T}{2\pi}\right]^{1/2}i\mathbf{k}e^{i\mathbf{k}\cdot\mathbf{r}}\beta\right]\nabla\phi'(\mathbf{r})-\frac{T}{2\eta}k^2\left[\alpha\beta-\frac{\alpha^2+\beta^2}{2}\right]+\frac{2z}{\xi^2}\cos\left[\left[\frac{2\pi}{T}\right]^{1/2}\tilde{\phi}(\mathbf{r})\right]. \tag{A10}$$

Thus

$$\frac{1}{\Omega}\frac{\partial}{\partial\alpha}\frac{\partial}{\partial\beta}\ln(Z'_{\alpha\beta})\bigg|_{\alpha=\beta=0}=\frac{T}{2\pi}\frac{1}{\Omega}\int d^2rd^2r'e^{-i\mathbf{k}\cdot(\mathbf{r}-\mathbf{r}')}k^2\langle\nabla\phi(\mathbf{r})\nabla\phi(\mathbf{r}')\rangle_{\mathrm{sG}}-\frac{T}{2\pi}k^2=\frac{T}{2\pi}k^4G(k)-\frac{T}{2\pi}k^2, \tag{A11}$$

where the last equality follows by partial integration. Combining Eqs. (A8) and (A11) gives

$$-\langle n(\mathbf{k})n(-\mathbf{k})\rangle=\frac{T}{2\pi}G(k)-\frac{T}{2\pi}k^2, \tag{A12}$$

which by aid of Eq. (3.6) turns into the well-known formula for linear screening

$$V_L(\mathbf{k})=\left[1-\frac{2\pi}{Tk^2}\langle n(\mathbf{k})n(-\mathbf{k})\rangle\right]\frac{2\pi}{k^2}. \tag{A13}$$

APPENDIX B

The calculation of $F=-(d/dr)V_L(r)$ goes as follows: $V_L(r)$ is given by the linear screening formula Eq. (3.10) so that

$$\frac{d}{dr}V_L(r)=\frac{d}{dr}\int\frac{d^2k}{2\pi}e^{i\mathbf{k}\cdot\mathbf{r}}\frac{2\pi}{k^2}\left[\int d^2r'e^{i\mathbf{k}\cdot\mathbf{r}}f(r')\right], \tag{B1a}$$

where

$$f(r)=\int\frac{d^2k}{(2\pi)^2}\left[1-\frac{2\pi}{k^2T}\langle n(\mathbf{k})n(-\mathbf{k})\rangle\right]e^{i\mathbf{k}\cdot\mathbf{r}}. \tag{B1b}$$

Do the angular integrations in Eq. (B1a) which give

$$\frac{d}{dr}V_L(r)=2\pi\frac{d}{dr}\int_0^\infty dr'dk\frac{r'}{k}J_0(kr)J_0(kr')f(r'), \tag{B2}$$

where J_n is the Bessel function of order n. Next use

$$\frac{d}{dz}J_0(z)=-J_1(z)$$

resulting in

$$\frac{d}{dr}V_L(r)=-2\pi\int_0^\infty dr'dk\,r'J_1(kr)J_0(kr')f(r'). \tag{B3}$$

The k integration may now be carried out using the formula[19]

$$\int_0^\infty dx\, J_1(\alpha x)J_0(\beta x)=\begin{cases}1/\alpha, & \beta<\alpha\\ 0, & \beta>\alpha\end{cases} \tag{B4}$$

which gives

$$\frac{d}{dr}V_L(r)=-\frac{2\pi}{r}\int_0^r dr'r'f(r') . \tag{B5}$$

Integrating Eq. (B1b) results in

$$f(r)=\delta(\mathbf{r})-\frac{1}{T}\int_0^\infty \frac{dk}{k}\langle n(\mathbf{k})n(-\mathbf{k})\rangle J_0(kr) . \tag{B6}$$

The Fourier transform of the charge-density correlation function may be written as

$$\begin{aligned}\langle n(\mathbf{k})n(-\mathbf{k})\rangle &= \int d^2r'e^{i\mathbf{k}\cdot\mathbf{r}}\langle n(r')n(0)\rangle\\ &=2\pi\int_0^\infty dr'r'J_0(kr')\langle n(r')n(0)\rangle\\ &=2\pi\int_0^\infty dr'r'[J_0(kr')-1]\langle n(r')n(0)\rangle ,\end{aligned} \tag{B7}$$

where in the last equality we have used the charge-neutrality condition $\int d^2rn(r)=0$. Thus $f(r)$ may be written as

$$f(r)=\delta(\mathbf{r})-\frac{2\pi}{T}\int_0^\infty dk\, dr'\frac{r'}{k}J_0(kr)[J_0(kr')-1] \times\langle n(r')n(0)\rangle . \tag{B8}$$

Inserted in Eq. (B5) this gives

$$\frac{d}{dr}V_L(r)=-\frac{1}{r}+\frac{4\pi^2}{Tr}\int_0^\infty dk\, dr'\left[\int_0^r d\tilde{r}\,\tilde{r}J_0(k\tilde{r})[J_0(kr')-1]\frac{r'}{k}\langle n(r')n(0)\rangle\right] . \tag{B9}$$

Next we use the formulas[19]

$$\int_0^a dx\, xJ_0(x)=aJ_1(a) , \tag{B10}$$

$$\int_0^\infty \frac{dx}{x^2}[J_0(ax)-1]J_1(bx)=\begin{cases}-\frac{b}{4}\left[1+2\ln\left[\frac{a}{b}\right]\right], & 0<b<a\\ -\frac{a^2}{4b}, & 0<a<b\end{cases} \tag{B11}$$

and express Eq. (B9) as

$$\begin{aligned}\frac{d}{dr}V_L(r)&=-\frac{1}{r}+\frac{4\pi^2}{T}\int_0^\infty \frac{dk}{k^2}dr'r'J_1(kr)[J_0(kr')-1]\langle n(r')n(0)\rangle\\ &=-\frac{1}{r}-\frac{\pi^2}{Tr}\int_0^r dr'(r')^3\langle n(r')n(0)\rangle-\frac{\pi^2}{T}r\int_r^\infty dr'r'[1+2\ln(r'/r)]\langle n(r')n(0)\rangle\\ &=-\left[\frac{1}{r\tilde{\epsilon}(r)}+\frac{\pi^2}{T}r\int_r^\infty dr'r'\langle n(r')n(0)\rangle+\frac{2\pi^2}{T}r\int_r^\infty dr'r'\ln\left[\frac{r'}{r}\right]\langle n(r')n(0)\rangle\right] ,\end{aligned} \tag{B12}$$

where in the last equality we have used the definition of $\tilde{\epsilon}(r)$ given by Eq. (2.18). The force between the test charges is $F=-\partial V_L(r)/\partial r$ and Eqs. (2.19) follow with F_1, F_2, and F_3 corresponding to the three terms on the right-hand side of (B12), respectively.

To produce the calculation of Eqs. (4.9) start with the length-dependent screening function $\tilde{\epsilon}(r)$ [Eq. (2.18)] and differentiate with respect to $l=\ln(r/\xi)$,

$$\frac{d}{dl}\frac{1}{\tilde{\epsilon}(l)}=\frac{\pi^2}{T}r^4\langle n(r)n(0)\rangle . \tag{B13}$$

Using Eqs. (4.6) and (4.8) it may be expressed as

$$\frac{d}{dl}\frac{1}{\tilde{\epsilon}(l)}=-\frac{2\pi^2 z(l)^2}{T} , \tag{B14}$$

which is Eq. (4.9a). Starting with Eq. (4.8) and differentiating gives

$$\frac{d}{dl}z(l)=\frac{z(l)}{2}\left[4-\frac{2rF(r)}{T}\right] , \tag{B15}$$

where $F(r)$ is the force acting between two infinitesimal test charges [see Eq. (B12)]. From Eq. (B12) one has

$$\frac{2rF(r)}{T}=\frac{2}{T\tilde{\epsilon}(l)}+A(l) , \tag{B16}$$

where

$$\begin{aligned}A(l)&=\frac{2\pi^2r^2}{T^2}\int_r^\infty dr'r'[1+2\ln(r'/r)]\langle n(r')n(0)\rangle\\ &=\frac{2r^2}{T}\int_r^\infty \frac{dr'}{r'^2}[1+2\ln(r'/r)]\frac{d}{dr'}\left[\frac{1}{\tilde{\epsilon}(r')}\right]\end{aligned} \tag{B17}$$

and Eq. (2.18) was used to obtain the last equality. Partial integration now gives

$$A(l) = -\frac{2}{T\tilde{\epsilon}(r)} + \frac{4r^2}{T}\int_r^\infty dr' \frac{\ln(r'/r)}{(r')^3}\frac{1}{\tilde{\epsilon}(r')} . \quad \text{(B18)}$$

Switching to a logarithmic length scale $l' = \ln(l'/\xi)$ and changing variables give

$$A(l) = -\frac{2}{T\tilde{\epsilon}(l)} + 4\int_l^\infty dl'(l'-l)e^{-2(l'-l)}\frac{1}{T\tilde{\epsilon}(l')}$$
$$= -\frac{2}{T\tilde{\epsilon}(l)} + \int_0^\infty dx\, xe^{-x}\frac{1}{T\tilde{\epsilon}(x/2+l)} . \quad \text{(B19)}$$

Insertion in Eq. (B16) yields

$$\frac{2rF(r)}{T} = \int_0^\infty dx\, xe^{-x}\frac{1}{T\tilde{\epsilon}(x/2+l)} . \quad \text{(B20)}$$

Now insert Eq. (B20) in Eq. (B15) and Eq. (4.9b) follows.

APPENDIX C

Start with Eqs. (4.9) and define

$$h(x) = \frac{d}{dx}\left[\frac{1}{T\tilde{\epsilon}(x)}\right] . \quad \text{(C1)}$$

The integral appearing in Eq. (4.9b) may by partial integration be rewritten as

$$\int_0^\infty dx\, e^{-x}x\frac{1}{T\tilde{\epsilon}(l+x/2)} = \frac{1}{T\tilde{\epsilon}(l)} + \tfrac{1}{2}\int_0^\infty dx\,(x+1)e^{-x}h(l+x/2) . \quad \text{(C2)}$$

From Eq. (4.9a) one has

$$h(l) = -\frac{2z^2(l)\pi^2}{T^2} . \quad \text{(C3)}$$

Combining this with Eq. (4.9b) and using Eq. (C2) gives

$$\frac{d}{dl}\ln[h(l)] = 4 - \frac{1}{T\tilde{\epsilon}(l)} - \tfrac{1}{2}\int_0^\infty dx(x+1)e^{-x}h(l+x/2) , \quad \text{(C4)}$$

which upon integration becomes

$$\ln\left[\frac{h(l)}{h(0)}\right] = \int_0^l dx\left[4 - \frac{1}{T\tilde{\epsilon}(x)}\right] - \tfrac{1}{2}\int_0^\infty dx(x+1)e^{-x}\left[\frac{1}{T\tilde{\epsilon}(l+x/2)} - \frac{1}{T\tilde{\epsilon}(x/2)}\right] . \quad \text{(C5)}$$

Partial integration of the terms on the right-hand side and exponentiation turns Eq. (C5) into

$$h(l) = h(0)\exp\left[\left[4 - \frac{1}{T\tilde{\epsilon}(l)}\right]l + \int_0^\infty dx\, xh(x) - \int_0^l dx\, h(x) - \tfrac{1}{4}\int_0^\infty dx\,(x+2)e^{-x}[h(l+x/2) - h(x/2)]\right] . \quad \text{(C6)}$$

One notes that

$$\frac{1}{T\epsilon(l)} = \frac{1}{T\tilde{\epsilon}(0)} + \int_0^l dx\, h(x)$$

and Eqs. (6.1) follow.

[1]J. M. Kosterlitz and D. J. Thouless, J. Phys. C **6**, 1181 (1973).

[2]V. L. Berezinskii, Zh. Eksp. Teor. Fiz. **61**, 1144 (1971) [Sov. Phys.—JETP **34**, 610 (1972)].

[3]P. Minnhagen, Phys. Rev. Lett. **54**, 2351 (1985).

[4]Some recent reviw articles are J. M. Kosterlitz and D. J. Thouless, in *Progress in Low Temperature Physics, Vol. VII B*, edited by D. F. Brewer (North-Holland, Amsterdam, 1978); B. I. Halperin, in *Physics of Low-Dimensional Systems, Proceedings of Kyoto Summer Institute, 1979*, edited by Y. Nagaoka and S. Hikami [Publications Office (Prog. Theor. Phys.), Kyoto, 1979], p. 53; D. R. Nelson, in *Fundamental Problems in Statistical Mechanics V*, edited by E. G. D. Cohen (North-Holland, Amsterdam, 1980), p. 53.

[5]T. Ohta and D. Jasnow, Phys. Rev. B **20**, 139 (1979).

[6]D. R. Nelson and J. M. Kosterlitz, Phys. Rev. Lett. **39**, 1201 (1977).

[7]P. Minnhagen and G. G. Warren, Phys. Rev. B **24**, 6758 (1981).

[8]J. M. Kosterlitz, J. Phys. C **7**, 1046 (1974).

[9]P. Minnhagen (unpublished).

[10]For a review, see P. Minnhagen, in *NATO Advanced Study Institute on Localization, Percolation and Superconductivity*, edited by A. M. Goldman and S. A. Wolf (Plenum, New York, 1984), p. 287.

[11]E. H. Hauge and P. C. Hemmer, Phys. Norv. **5**, 209 (1971).

[12]A. P. Young, J. Phys. C **11**, L453 (1978); A. P. Young, in *NATO Advanced Study Institute on Ordering in Strongly Fluctuating Condensed Matter System*, edited by T. Riste (Plenum, New York, 1980), p. 271.

[13]P. Minnhagen and M. Nylén, Phys. Rev. B **31**, 5768 (1985).

[14]J. V. José, L. P. Kadanoff, S. Kirkpatrick, and D. R. Nelson, Phys. Rev. B **16**, 1217 (1977).

[15]P. B. Wiegmann, J. Phys. C **11**, 1583 (1978).

[16]D. J. Amit, Y. Y. Goldschmidt, and G. Grinstein, J. Phys. A **13**, 585 (1980).

[17]A. M. Polyakov, Nucl. Phys. **B20**, 429 (1977); S. Samuel, Phys. Rev. D **18**, 1916 (1978).

[18]Further details may be found in P. Minnhagen, NORDITA

Report No. 80/25 (unpublished). P. Minnhagen, Phys. Rev. B **23**, 5745 (1981).

[19]I. S. Gradshteyn and M. Ryzhik, *Tables of Integrals, Series and Products* (Academic, New York, 1980); formulas 6.512.3, 6.561.5, and 6533.3 are used in Appendix B, formula 3.613.2 in Sec. V.

[20]It would be interesting to compare the relation between the RG equations and the new equations in more detail like, e.g., a term by term comparison for an expansion of the critical line close to $T=\frac{1}{4}$. However, such a comparison presumes that both sets of equations are derived with precisely the same ultraviolet cutoff prescription. This presumption makes such a comparison a somewhat nontrivial problem.